Original Article

Grayscale ultrasound feature typing of metastatic ovarian tumors, particularly signet-ring cell carcinoma

Junying Liu[1,2], Cai Chang[1,2], Haixian Zhang[1,2]^

[1]Department of Ultrasound, Fudan University Shanghai Cancer Center, Shanghai, China; [2]Department of Oncology, Shanghai Medical College, Fudan University, Shanghai, China

Contributions: (I) Conception and design: All authors; (II) Administrative support: All authors; (III) Provision of study materials or patients: J Liu, C Chang; (IV) Collection and assembly of data: H Zhang, J Liu; (V) Data analysis and interpretation: All authors; (VI) Manuscript writing: All authors; (VII) Final approval of manuscript: All authors.

Correspondence to: Haixian Zhang. Department of Ultrasound, Fudan University Shanghai Cancer Center, Shanghai Medical College, Fudan University, 270 Dong'an Rd, Xuhui District, Shanghai 200032, China. Email: 14111220032@fudan.edu.cn.

Background: To describe grayscale ultrasound (US) features of metastatic ovarian tumors (MOTs) based on origin of the primary tumor in a large sample size study.

Methods: This retrospective cross-sectional single-center study included 112 patients with 190 histopathologically confirmed MOTs. Among the patients, 102 collectively had 144 masses, which were detected via US. The clinical data and static US images of MOTs were collected.

Results: The MOTs were mostly bilateral (78.9%) but had a lower rate of bilaterality when detected by US (55.6%). Breast cancer metastasis had the highest nondetection rate (69.6%), because its focal metastasis could only be recognized using histology or immunohistochemistry. The stomach was the most common origin of metastasis (45.3% and 50.7% detected via pathology and US, respectively). The US images were classified into three subtypes: multilocular solid (Type A), purely solid (Type B), and solid with several round or oval cysts (Type C). The MOTs that originated from the colon mostly belonged to Type A (65.1%) and closely mimicked primary epithelial ovarian tumor morphologically. The MOTs that originated from the stomach predominantly belonged to Types B (31.5%) and C (57.5%). Signet-ring cell carcinoma (SRCC) corresponded to Types B and C regardless of origin.

Conclusions: The developed novel typing method provides more vivid images for classifying MOTs compared with existing typing methods. Given that no specific sonographic parameters have been established to distinguish MOTs from primary invasive ovarian tumors, these images may be helpful in diagnosing these masses.

Keywords: Metastatic ovarian tumor (MOT); subtype; signet-ring cell carcinoma (SRCC); ultrasound

Submitted Nov 27, 2021. Accepted for publication Sep 09, 2022. Published online Oct 08, 2022.
doi: 10.21037/qims-21-1149
View this article at: https://dx.doi.org/10.21037/qims-21-1149

^ ORCID: 0000-0002-2374-2491.

Introduction

The ovary is a relatively frequent site of metastases. About 5–20% of ovarian masses are metastases from other malignant tumors, such as gastrointestinal tumors, breast cancer, and gynecological tumors (1-3). Primary ovarian cancer must be distinguished from metastatic ovarian tumor (MOT), because this clinical information is crucial in devising appropriate treatment strategies and establishing prognosis (4-6). Ultrasound (US) is advantageous because of its accessibility as a first-line imaging examination that is painless and relatively inexpensive compared with computed tomography (CT), magnetic resonance imaging (MRI), and positron emission tomography (PET). Few studies have specifically compared the characteristics of metastatic ovarian malignancies of different origins (7-13). Such studies have reported that metastases in the ovaries are either predominantly or completely solid, but have failed to note specific sonographic features that characterize metastatic lesions.

As observed in routine clinical examination, most cases of solid metastases in the ovary are signet-ring cell carcinoma (SRCC), a special type of mucinous carcinoma characterized by a purely solid mass or a solid mass with one to several round or oval cysts. These observations prompted us to conduct a thorough investigation of the prevalence of this feature in a series of MOTs. We present the following article in accordance with the STROBE reporting checklist (available at https://qims.amegroups.com/article/view/10.21037/qims-21-1149/rc).

Methods

Patients

This was a retrospective cross-sectional single-center study. The study was conducted in accordance with the Declaration of Helsinki (as revised in 2013). The Independent Ethics Committee of Shanghai Cancer Center, Fudan University (Shanghai, China) approved this study, and individual consent for this retrospective analysis was waived. Clinical data and static US images of patients with MOTs, who underwent surgery from January 2010 to December 2019, were collected. *Figure 1* shows the patient selection flowchart. The inclusion criteria were as follows: (I) ovarian US was performed before surgery, and (II) MOTs had been pathologically proven. The exclusion criteria were as follows: (I) primary ovarian cancer, (II) ovarian lesion without definite pathological diagnosis, and (III) MOTs without definite primary origin. Patient MOT data were collected, even for cases whose MOT lesions were not detectable by US. A total of 190 masses from 112 patients were assessed.

Data collection and image classification

The medical records of the included cases were reviewed to obtain the following information: patient age, primary origin of tumor, chronology of onset, and pathological analysis. Static US images were obtained via transabdominal or transvaginal US using a routine standardized examination technique. The frequency of the transvaginal probes varied between 5.0 and 9.0 MHz, and that of the abdominal probes between 3.5 and 5.0 MHz. Transvaginal US is advantageous when the MOTs are small or located in the lower pelvis. During transvaginal US, the transvaginal probe is placed into the patient's vagina and pressed close to the cervix. Otherwise, transabdominal US is preferable, as the transabdominal probe can scan the whole abdomen and pelvis. The collected images were evaluated by an image interpretation committee. The committee comprised three gynecological oncology US specialists from the Shanghai Cancer Center. Two of these had 10 years of experience, and the other one had 20 years of experience. The US images of each lesion were first analyzed by at least two members of the committee. When interpretation was difficult, the images were evaluated by a third member.

The masses detected by US were classified into three subtypes (*Figure 2*). Type A mimicked primary epithelial ovarian tumor and consisted of multilocular solid masses with variable ratios of solid and cystic components and good US penetration. Type B comprised purely solid masses with inner echo, which could be uniform or not. Type C consisted of solid masses with round or oval cysts, which are plump, have smooth walls and good inner US penetration, and are of variable number, size, and position (*Figure 3*). Their shape is mostly regular, but sometimes it can be irregular or polylobate; their size can be large, and they can be adherent to peripheral tissues.

Statistical analysis

Statistical analyses were performed using SPSS version 22.0 for Windows (IBM Corp., Armonk, NY, USA). We conducted χ^2 tests to analyze categorical variables. Statistical significance was set at $P<0.05$.

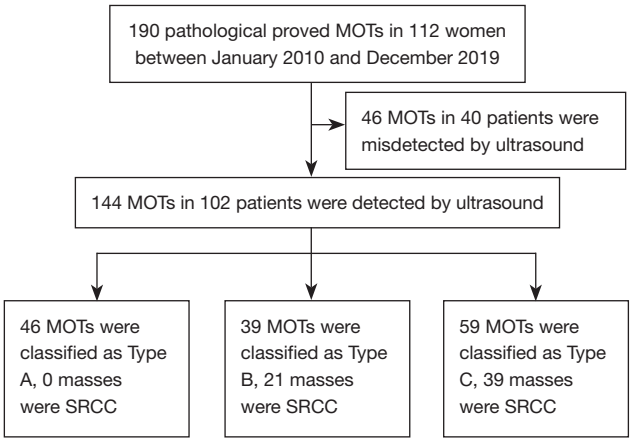

Figure 1 Patient selection flowchart. MOTs, metastatic ovarian tumor; SRCC, signet-ring cell carcinoma.

Results

Between January 2010 and December 2019, 190 MOTs in 112 women were surgically treated. Among these, 144 (75.8%) MOTs in 102 women (91.1%) were detected by US. The age of the 102 women was in the range of 26 to 78 years (mean age: 48±11.2 years). The sites of primary tumor histological diagnoses included the stomach, colon, breast, uterus, liver-pancreas-biliary (LPB) tract, appendix, lungs, and kidneys (*Table 1*). Except for one uterine endometrial stromal sarcoma and one uterine neuroendocrine carcinoma, the 144 masses in the US-detected group were classified as adenocarcinoma, including 73 gastric adenocarcinomas, 43 colorectal adenocarcinomas, 6 breast invasive ductal carcinomas,

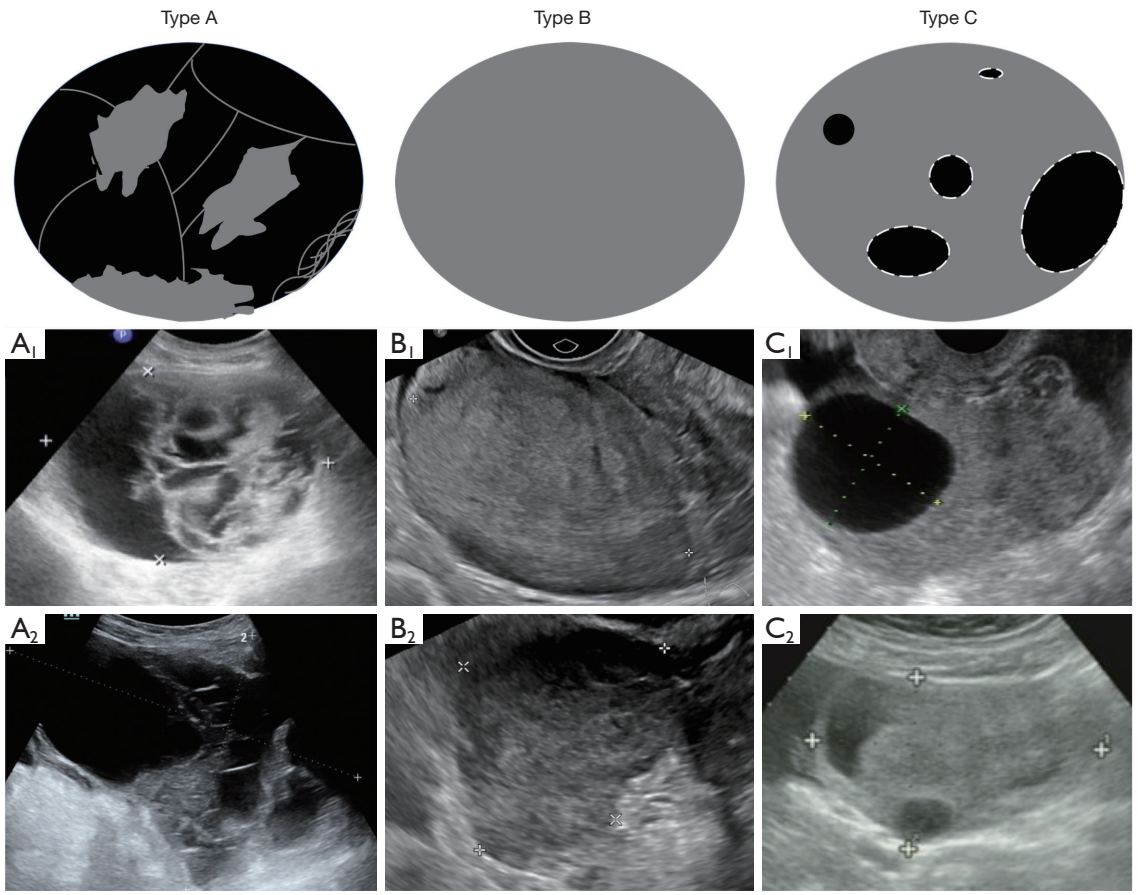

Figure 2 Schematic diagram of the three subtypes of MOTs. Typical type A (multilocular solid) appearance of metastasis from colon cancer (A1) and bile duct cancer (A2). Typical type B (purely solid) appearance of metastasis from stomach cancer (B1) and uterine neuroendocrine carcinoma (B2). Typical type C (solid with round or oval cysts) appearance of metastasis from stomach cancer (C1) and appendix cancer (C2). MOTs, metastatic ovarian tumors.

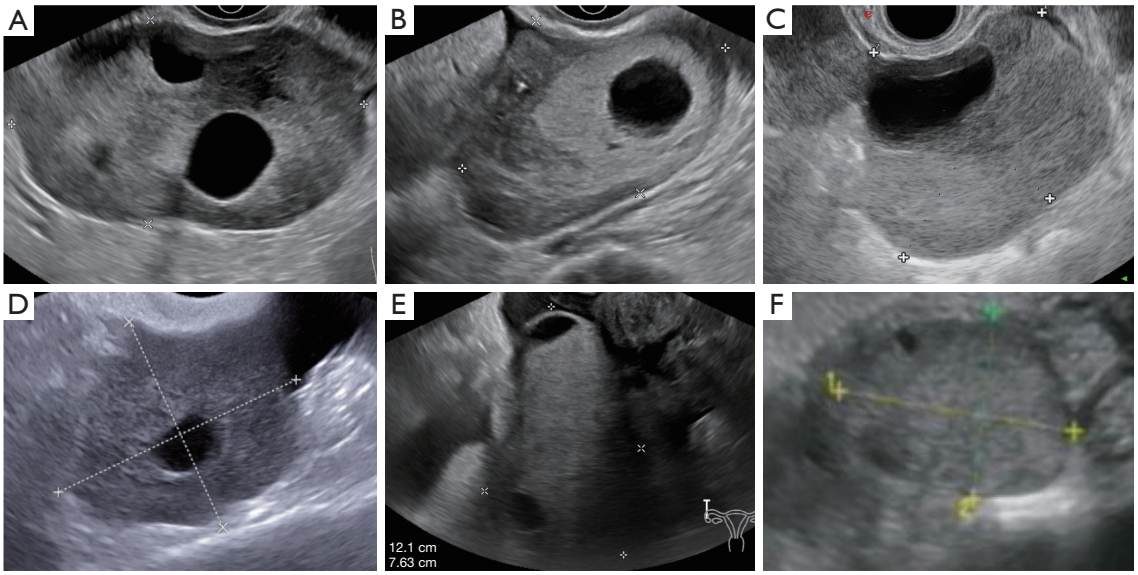

Figure 3 Typical images of type C masses. The cyst is round and has a smooth wall, superior transparency, and a variable number, size, and position. (A) MOT from gastric adenocarcinoma of a 51-year-old woman. (B) MOT from gastric adenocarcinoma of a 49-year-old woman. (C) MOT from ascending colon adenocarcinoma of a 42-year-old woman. (D) MOT from breast lobular carcinoma of a 51-year-old woman. (E) MOT from gastric adenocarcinoma of a 52-year-old woman. (F) MOT from gastric adenocarcinoma of a 41-year-old woman. MOT, metastatic ovarian tumor.

1 invasive lobular carcinoma, 2 cervical adenocarcinomas, 2 uterine endometrial adenocarcinomas, 1 gallbladder adenocarcinoma, 2 cholangiocarcinomas, 3 pancreatic ductal adenocarcinomas, 6 appendicular adenocarcinomas, 1 lung adenocarcinoma, and 2 renal clear cell carcinomas.

Metastasis was identified before primary tumor diagnosis in 12 patients. Metastasis and primary tumors were simultaneously identified in 16 patients. Metastasis was identified after primary tumor diagnosis in 85 patients, and the time interval ranged from 1 month to 186 months [median: 18 months, interquartile range (IQR): 11.5 to 29 months; *Table 2*]. One patient had a unilateral MOT detected before a primary gastric cancer was found and then underwent gastric surgery and unilateral MOT surgery prior to the discovery of another MOT on the other side 7 months later.

The most common origin of MOTs was the stomach (45.3% and 50.7% via pathology and US, respectively). Breast origin had the highest nondetection rate (69.6%). In the nondetection group, unilateral nondetection of bilateral metastasis was found in 31 patients, unilateral nondetection of unilateral metastasis occurred in 2 patients, and bilateral nondetection of bilateral metastasis occurred in 6 patients. (*Table 3*). No significant difference in age was observed between the US-detected and US-undetected groups (P=0.770). The maximum tumor diameter of the US-undetected group was significantly smaller than that of the US-detected group (P<0.05, *Table 4*).

The masses that originated from the colon were mostly multilocular and solid (Type A; 28/43, 65.1%). Those that originated from the stomach (65/73 in total, 89.0%) were mostly solid and could be classified as Types B (23/73, 31.5%) and C (42/73, 57.5%). Furthermore, 60 SRCC cases were found, and their US features could be classified into Types B and C regardless of their origin (stomach, colon, gall bladder, or appendix) (*Table 5*). A total of 68.5% (50/73) MOTs that originated from the stomach were SRCCs (23.2% features Type B, 45.2% features Type C).

Discussion

The histology of MOTs usually corresponds to that of the primary tumor. de Waal *et al.* reported that the histological type of the primary tumors of the gastrointestinal tract that had metastasized to the ovaries was most frequently adenocarcinoma (97%), and ductal invasive carcinoma was the histological type of breast cancer that gave rise to most ovarian metastases (41%) (14). Lewis *et al.*

Table 1 Primary histopathology of metastatic ovarian tumors

Primary histopathology	Pathology detected	US detected	US undetected
Stomach			
Adenocarcinoma	86/58*	73/50*	13/8*
Colon			
Adenocarcinoma	54/6*	43/6*	11
Breast			
Invasive ductal carcinoma	20	6	14
Invasive lobular carcinoma	3	1	2
Uterus			
Cervical adenocarcinoma	2	2	0
Endometrial adenocarcinoma	2	2	0
Cervical squamous carcinoma	1	0	1
Endometrial stromal sarcoma	2	1	1
Neuroendocrine carcinoma	2	1	1
L-P-B tract			
Gallbladder adenocarcinoma	2/2*	1/1*	1/1*
Cholangiocarcinoma	2	2	0
Pancreatic adenocarcinoma	3	3	0
Appendix			
Adenocarcinoma	7/3*	6/3*	1
Lung			
Adenocarcinoma	2	1	1
Kidney			
Clear cell carcinoma	2	2	0
Total	190/69*	144/60*	46/9*

Marked with *: cases of SRCC. US, ultrasound; L-P-B, liver-pancreas-biliary; SRCC, signet-ring cell carcinoma.

Table 2 Chronology of primary tumors and at various sites

Primary location	Metastasis first	Synchronous	Primary first [Min–Max] {Median (IQR)}
Stomach[#]	8	7	35 [1–180] {16 (10.5, 23.5)}
Colon	1	2	31 [4–120] {17 (12.0, 29.0)}
Breast	0	0	13 [6–186] {33 (12.0, 60.0)}
Uterus	1	3	1 [16]
LPB tract	2	0	2 [11, 23]
Appendix	0	4	0
Lung	0	0	1 [18]
Kidney	0	0	2 [20, 83]
Total	12	16	85 [1–186] {18 (11.5, 29.0)}

[Min–Max]: time interval (month) between primary tumors and MOTs. {Median (IQR)}: median time interval (month) between detection of primary tumor and metastasis. Marked with [#]: one patient had unilateral MOT first before primary gastric cancer and then had gastric surgery and unilateral MOT surgery before MOT was found 7 months later on the other side. Min, minimum; Max, maximum; IQR, interquartile range; MOT, metastatic ovarian tumor; LPB, liver-pancreas-biliary.

Table 3 Bilaterality of pathology and US-detected MOTs

Origins	Pathological detected		US detected		US undetected	
	Cases	Bilaterality	Cases	Bilaterality	Cases	Bilaterality
Stomach	86 (45.3%)	72[§]	73 (50.7%)	48[§]	13 (15.1%)	0
Colon	54 (28.4%)	38[§]	43 (29.9%)	20[§]	11 (20.4%)	0
Breast	23 (12.1%)	20	7 (4.9%)	2	16 (69.6%)	12
Uterus	9 (4.7%)	8	6 (3.2%)	4	3 (33.3%)	0
LPB tract	7 (3.7%)	6	6 (3.2%)	4	1 (14.3%)	0
Appendix	7 (3.7%)	6[¶]	6 (3.2%)	4	1 (14.3%)	0
Lung	2 (1.1%)	2	1 (0.7%)	0	1 (50%)	0
Kidney	2 (1.1%)	0	2 (1.4%)	0	0	0
Total	190	150	144	80	46 (24.2%)	12

Marked with [§]: one patient had unilateral ovarian metastatic mass surgery twice within a 1-year interval. Marked with [¶]: one patient had a previous unilateral oophorectomy for unknown reasons. US, ultrasound; MOTs, metastatic ovarian tumors; LPB, liver-pancreas-biliary.

Table 4 Patient age and mass diameter distribution of MOTs

Patients/masses	Age (years) (mean ± SD)	Maximum diameter (mm) (mean ± SD)		
		Left	Right	Both
Pathological detected (112/190)	26–78 (47.4±11.0)	6–250 (74.9±52.7)	20–238 (86.0±49.6)	6–250 (81.2±52.0)
US detected (102/144)	26–78 (48.0±11.1)	20–250 (89.4±52.7)	20–238 (94.4±48.7)	20–238 (92.0±50.5)
US undetected (38/46)	32–73 (47.7±10.9)	6–80 (33.8±16.1)*	20–70 (37.2±13.3)*	6–80 (33.8±15.9)*

Marked with *: $P<0.05$ compared with ultrasound detected group. MOT, metastatic ovarian tumor; SD, standard deviation; US, ultrasound.

Table 5 Primary tumor origins of MOTs with different US subtypes

Subtype	Stomach	Colon	Breast	Uterus	LPB tract	Appendix	Lung	Kidney	Total
A	8	28	2	3	3	2	0	0	46
B	23/17*	6/2*	2	3	1/1*	1/1*	1	2	39/21*
C	42/33*	9/4*	3	0	2	3/2*	0	0	59/39*
Total	73/50*	43/6*	7	6	6/1*	6/3*	1	2	144/60*

Marked with* cases of SRCC. MOTs, metastatic ovarian tumors; US, ultrasound; LPB, liver-pancreas-biliary; SRCC, signet-ring cell carcinoma.

detailed and analyzed clinical and pathologic features of 86 cases of ovarian involvement of metastatic colorectal adenocarcinoma (15). In our series of 144 US-detected MOTs, 142 (98.6%) were adenocarcinomas, which is consistent with previous studies.

Colorectal metastases are difficult to differentiate from primary ovarian cancer via US and microscopy (16,17). We confirmed this observation in our relatively large study population, where 65.1% (28/43) of the colorectal metastases closely mimicked primary epithelial ovarian tumor morphologically (Type A). In this case, immunohistochemistry plays a major role in distinguishing primary from secondary ovarian tumors and may suggest the potential primary tumor site. The bilaterality characteristics agreed fairly well with the descriptions of MOTs in pathology textbooks. However, the detection rate

of bilaterality using US was low. We speculated two possible reasons why metastatic tumors were not detected. First, the ovary was largely normal; therefore, detection via imaging was difficult. In these cases, focal metastasis was identified using histologic examination and immunohistochemistry, and this mostly occurred in breast cancer metastases. The latter observation is consistent with findings from a previous study (18), which found six cases of breast cancer-related ovariectomy. Second, the contralateral mass was too large and thus obstructed smaller masses. The maximum bilateral diameter ratio ranged from 1.3 to 14.2 (3.4±2.4).

Previous studies have classified metastatic tumors into solid, multilocular solid, or at least unilocular solid and not purely unilocular or multilocular masses based on US characteristics (17,19-22). This classification is too broad and does not provide proper schematic images for reference. A vivid schematic image can assist radiologists to identify MOTs, especially in the case of inexperienced radiologists and MOTs on first presentation. In addition to indicating the possibility of MOTs, the subtype predicts the origins of MOTs. Knowledge of the subtype of MOTs before surgery is highly likely to improve patient triage, and it also makes it possible to optimize treatment. In the present study, we classified metastatic tumors into three different subtypes (A, B, and C), which provide more vivid US images for reference. Aside from the commonly described multilocular solid (Type A) and purely solid (Type B) tumors, we described a novel sonographic feature of solid ovarian metastasis morphology, that is, Type C, which is characterized by a solid tumor with one or several round or oval cysts, that are plump and have a smooth wall and superior transparency. The cyst lumens contain a clear, mucinous, or hemorrhagic fluid. The presumed pathological reason is the presence of glands, many of which include dilated cysts, punctuate the peripheral cellular component, and are more conspicuous in the edematous central component. Guerriero *et al.* (23) reported a cystic component in 39% of solid metastatic ovarian cases, but they did not further explain these cases. In our study, this sonographic characteristic was readily recognizable and present in 41.7% (60/144) of the metastatic tumors. Furthermore, the metastatic SRCC in the ovary featured Type B and C characteristics regardless of their origin (stomach, colon, gall bladder, or appendix), and no metastatic SRCC featured Type A characteristics. Moreover, primary ovarian tumors with signet-ring cells are rare (16,24,25), and the prognosis is especially unfavorable if the primary histology of MOT is SRCC (26). Based on these observations, when an ovarian mass features Type B or Type C, not only should MOTs be taken into consideration but also SRCC, especially in patients with stomach carcinoma.

Although the relatively large number of cases included in our study permitted quite an accurate analysis of the different parameters of each group, the present study had some limitations. First, the sample size was relatively small, despite that data collection was conducted over 10 years. Except MOTs that originated from the stomach and colon, the single digits of MOTs that originated from the breast, uterus, LPB, appendix, lung, and kidney might be unrepresentative, as such, the results should be considered observational. Thus, more cases are needed for validation. Second, the patients enrolled in the study were diagnosed using US, and CT- or MRI-diagnosed MOTs without US diagnosis were not included; therefore, selection bias was unavoidable. Third, the collected static US images only reflect several typical sections of MOTs, which may have introduced a certain amount of subjectivity. Fourth, the static US images obtained during the past 10 years were collected from different US machines; hence, the image quality might not be consistent. Finally, no color Doppler flow imaging (CDFI) analysis was conducted because of the inconsistency of such imaging of the tumor vascularity using different US machines. Despite these factors, we took several measures to optimize data quality. (I) The cancer center through which patients were recruited has been admitting patients with all kinds of malignant tumors, and thus included as many MOTs as possible. (II) Data collection started in 2010, when high-definition US machines were available, which could gather high-definition US images. (III) An image interpretation committee was established to standardize the assessment criteria used for evaluation.

Conclusions

In summary, although US has certain nondetection rate because of the focal metastasis or high bilateral diameter ratio of some MOTs, we tested a novel US typing method, which provides more vivid images for classifying MOTs compared with existing typing methods and was found to be helpful when diagnosing MOTs.

Acknowledgments

Funding: This work was supported by the National Nature Science Foundation of China (Nos. 81901749

and 81801701) and the Shanghai Sailing Program (No. 19YF1410000).

Footnote

Reporting Checklist: The authors have completed the STROBE reporting checklist. Available at https://qims.amegroups.com/article/view/10.21037/qims-21-1149/rc

Conflicts of Interest: All authors have completed the ICMJE uniform disclosure form (available at https://qims.amegroups.com/article/view/10.21037/qims-21-1149/coif). The authors have no conflicts of interest to declare.

Ethical Statement: The authors are accountable for all aspects of the work in ensuring that questions related to the accuracy or integrity of any part of the work are appropriately investigated and resolved. The study was conducted in accordance with the Declaration of Helsinki (as revised in 2013). The present study was approved by the Independent Ethics Committee of Shanghai Cancer Center, Fudan University (Shanghai, China), and individual consent for this retrospective analysis was waived.

References

1. Simons M, Bolhuis T, De Haan AF, Bruggink AH, Bulten J, Massuger LF, Nagtegaal ID. A novel algorithm for better distinction of primary mucinous ovarian carcinomas and mucinous carcinomas metastatic to the ovary. Virchows Arch 2019;474:289-96.
2. Kir G, Gurbuz A, Karateke A, Kir M. Clinicopathologic and immunohistochemical profile of ovarian metastases from colorectal carcinoma. World J Gastrointest Surg 2010;2:109-16.
3. Lee SJ, Bae JH, Lee AW, Tong SY, Park YG, Park JS. Clinical characteristics of metastatic tumors to the ovaries. J Korean Med Sci 2009;24:114-9.
4. Bray F, Ferlay J, Soerjomataram I, Siegel RL, Torre LA, Jemal A. Global cancer statistics 2018: GLOBOCAN estimates of incidence and mortality worldwide for 36 cancers in 185 countries. CA Cancer J Clin 2018;68:394-424.
5. Johnson N, Bryant A, Miles T, Hogberg T, Cornes P. Adjuvant chemotherapy for endometrial cancer after hysterectomy. Cochrane Database Syst Rev 2011;(10):CD003175.
6. Williams MG, Bandera EV, Demissie K, Rodríguez-Rodríguez L. Synchronous primary ovarian and endometrial cancers: a population-based assessment of survival. Obstet Gynecol 2009;113:783-9.
7. Kurokawa R, Nakai Y, Gonoi W, Mori H, Tsuruga T, Makise N, Ushiku T, Abe O. Differentiation between ovarian metastasis from colorectal carcinoma and primary ovarian carcinoma: Evaluation of tumour markers and "mille-feuille sign" on computed tomography/magnetic resonance imaging. Eur J Radiol 2020;124:108823.
8. Tsili AC, Naka C, Argyropoulou MI. Multidetector computed tomography in diagnosing peritoneal metastases in ovarian carcinoma. Acta Radiol 2021;62:1696-706.
9. Kato MK, Shida D, Yoneoka Y, Yoshida H, Miyasaka N, Kanemitsu Y, Kato T. Novel classification of ovarian metastases originating from colorectal cancer by radiological imaging and macroscopic appearance. Int J Clin Oncol 2020;25:1663-71.
10. Auekitrungrueng R, Tinnangwattana D, Tantipalakorn C, Charoenratana C, Lerthiranwong T, Wanapirak C, Tongsong T. Comparison of the diagnostic accuracy of International Ovarian Tumor Analysis simple rules and the risk of malignancy index to discriminate between benign and malignant adnexal masses. Int J Gynaecol Obstet 2019;146:364-9.
11. Moro F, Pasciuto T, Djokovic D, Di Legge A, Granato V, Moruzzi MC, Mancari R, Zannoni GF, Fischerova D, Franchi D, Scambia G, Testa AC. Role of CA125/CEA ratio and ultrasound parameters in identifying metastases to the ovaries in patients with multilocular and multilocular-solid ovarian masses. Ultrasound Obstet Gynecol 2019;53:116-23.
12. Han S, Woo S, Suh CH, Lee JJ. Performance of pre-treatment ^{18}F-fluorodeoxyglucose positron emission tomography/computed tomography for detecting metastasis in ovarian cancer: a systematic review and meta-analysis. J Gynecol Oncol 2018;29:e98.
13. Ohliger MA, Hope TA, Chapman JS, Chen LM, Behr SC, Poder L. PET/MR Imaging in Gynecologic Oncology.

Magn Reson Imaging Clin N Am 2017;25:667-84.
14. de Waal YR, Thomas CM, Oei AL, Sweep FC, Massuger LF. Secondary ovarian malignancies: frequency, origin, and characteristics. Int J Gynecol Cancer 2009;19:1160-5.
15. Lewis MR, Deavers MT, Silva EG, Malpica A. Ovarian involvement by metastatic colorectal adenocarcinoma: still a diagnostic challenge. Am J Surg Pathol 2006;30:177-84.
16. McCluggage WG. Metastatic Neoplasms Involving the Ovary. Surg Pathol Clin 2011;4:297-330.
17. Stukan M, Alcazar JL, Gębicki J, Epstein E, Liro M, Sufliarska A, Szubert S, Guerriero S, Braicu EI, Szajewski M, Pietrzak-Stukan M, Fischerova D. Ultrasound and Clinical Preoperative Characteristics for Discrimination Between Ovarian Metastatic Colorectal Cancer and Primary Ovarian Cancer: A Case-Control Study. Diagnostics (Basel) 2019;9:210.
18. Karaosmanoglu AD, Onur MR, Salman MC, Usubutun A, Karcaaltincaba M, Ozmen MN, Akata D. Imaging in secondary tumors of the ovary. Abdom Radiol (NY) 2019;44:1493-505.
19. Ciccarone F, Codecà C, Versace V, Moro F. Ultrasound, macroscopic and histological features of malignant ovarian tumors. Metastatic tumors to the ovary: ovarian metastases from biliary tract and ovarian metastases from colon cancer. Int J Gynecol Cancer 2021;31:1388-90.
20. Andreotti RF, Timmerman D, Strachowski LM, Froyman W, Benacerraf BR, Bennett GL, Bourne T, Brown DL, Coleman BG, Frates MC, Goldstein SR, Hamper UM, Horrow MM, Hernanz-Schulman M, Reinhold C, Rose SL, Whitcomb BP, Wolfman WL, Glanc P. O-RADS US Risk Stratification and Management System: A Consensus Guideline from the ACR Ovarian-Adnexal Reporting and Data System Committee. Radiology 2020;294:168-85.
21. Moro F, Pozzati F, Mascilini F, Magoga G, Pasciuto T, Zannoni G, Scambia G, Testa AC. Ultrasound characteristics of ovarian metastases from low-grade appendiceal mucinous neoplasms. Ultrasound Obstet Gynecol 2018;51:699-700.
22. McCluggage WG. My approach to and thoughts on the typing of ovarian carcinomas. J Clin Pathol 2008;61:152-63.
23. Guerriero S, Alcazar JL, Pascual MA, Ajossa S, Olartecoechea B, Hereter L. Preoperative diagnosis of metastatic ovarian cancer is related to origin of primary tumor. Ultrasound Obstet Gynecol 2012;39:581-6.
24. Joshi VV. Primary Krukenberg tumor of ovary. Review of literature and case report. Cancer 1968;22:1199-207.
25. McCluggage WG, Young RH. Primary ovarian mucinous tumors with signet ring cells: report of 3 cases with discussion of so-called primary Krukenberg tumor. Am J Surg Pathol 2008;32:1373-9.
26. Yang XF, Yang L, Mao XY, Wu DY, Zhang SM, Xin Y. Pathobiological behavior and molecular mechanism of signet ring cell carcinoma and mucinous adenocarcinoma of the stomach: a comparative study. World J Gastroenterol 2004;10:750-4.

Cite this article as: Liu J, Chang C, Zhang H. Grayscale ultrasound feature typing of metastatic ovarian tumors, particularly signet-ring cell carcinoma. Quant Imaging Med Surg 2023;13(1):49-57. doi: 10.21037/qims-21-1149

